SERI/TP-34-169

CONF-790808--17

PERFORMANCE CHARACTERISTICS OF A COMMERCIALLY AVAILABLE POINT-FOCUS SOLAR POWER SYSTEM

MARK BOHN

APRIL 1979

TO BE PRESENTED AT THE
ASME/AICHE HEAT TRANSFER CONFERENCE
AUGUST 1979

Solar Energy Research Institute

1536 Cole Boulevard
Golden, Colorado 80401

A Division of Midwest Research Institute

Prepared for the
U.S. Department of Energy
Contract No. EG-77-C-01-4042

DISCLAIMER

NOTICE

Performance Characteristics of a Commercially Available, Point-Focus, Solar Power System

Mark Bohn

ABSTRACT

The performance of a commercially available solar electric power system is described in terms of instantaneous electrical power output for a given insolation and electrical energy production per day.

Receiver thermal loss coefficient and concentrator optical efficiency are measured and system performance is then given with steam cycle efficiency and electrical generator efficiency as parameters. System performance is limited by a relatively low optical efficiency of 44%. For peak insolation, this collector delivers 9.2 kw_{th} to the steam engine, representing 35% of the solar input.

THIS PAGE INTENTIONALLY LEFT BLANK

INTRODUCTION

Solar energy systems designed to deliver low grade energy have been commercially available for some time and are currently available from a large number of manufacturers. Such systems are used typically for domestic hot water and home heating, and there are some applications in cooling and refrigeration. The energy is collected by flat-plate collectors and is usually limited to temperatures of 100° C.

Somewhat higher temperatures (100° to 300° C.) can be achieved by concentrating collectors that focus the energy in one dimension (line focusing). An example is the parabolic trough collector, and several manufacturers are producing such collectors for applications primarily in process heat.

Efficient generation of electricity requires solar energy to be delivered at temperatures well above 300° C. and this requires focusing in two dimensions (point focusing) to produce higher levels of concentration and low thermal losses. At present, there is only one commercially available solar energy system that produces electrical power from solar energy through thermal conversion.

Solar Energy Research Institute, Golden, CO.

Due to the wide availability and application of systems designed for low grade energy delivery, a great deal of work has been done to assess performance of such systems (1 through 6). The purpose of this paper is to examine the performance of the one solar power system that is commercially available.

This solar power system is manufactured by the Omnium-G Company of Anaheim, Calif., and is based on a parabolic dish with a 6-meter diameter, 4-meter focal length, and geometric concentration ratio of 3600. Closed-loop sun tracking in both elevation and azimuth are provided, as well as automatic sun acquisition at sunrise. Solar energy is focused in a cavity receiver (aperture = 10 cm) and converted to thermal energy in the form of superheated steam. The steam is expanded in a Rankine cycle (piston engine) which in turn powers a 240-V., 60-Hz., 3-phase generator. The manufacturer claims a 7.5-$k\bar{w}_{e}$ output at peak insolation levels, with output power peaks up to the rated generator capacity of 10 $k\bar{w}_{e}$ for short periods.

In late 1978 the Solar Energy Research Institute (SERI) acquired two Omnium-G (O.G.) systems for installation at the SERI field test site in Golden, Colo. A broad range of tests are planned for these systems, including performance measurements of the systems, detailed

measurements of the optical characteristics of the collectors, detailed measurements of the thermal characteristics of the high temperature portions of the steam loop, and assessment of the viability of a distributed system of O.G. dishes. Finally, the dishes will be used as test beds for advanced receiver development.

In this paper we report on the first of the experiments: the performance evaluation of the delivered system. Power systems of this type have immediate commercial application in remote areas and at the ends of existing power grids. Thus, the need exists for performance evaluation so that potential users can determine if the system is economically viable in a given application.

System performance is given in terms of instantaneous electrical power output P_e for a given level of beam insolation I_o. This enables a potential user to determine expected output at a given location using local insolation values and local weather (cloudiness) data. For example, the electrical energy delivered per day in Golden is calculated from the $P_e(I_o)$ curve and local insolation data for one winter day.

System performance was determined by measuring two quantities associated with the ability of the concentrator and receiver to convert solar energy into thermal energy and to deliver this energy to the steam engine. These two quantities are the optical efficiency and the thermal loss of the high-temperature portions of the steam loop. The efficiencies of the steam engine and electrical generator then become parameters which determine the electrical power output.

In the following sections the determination of the electrical power output from the thermal losses and the optical efficiency is described. Next, the measurement of the thermal losses and optical efficiency is described. The resulting electrical power output is then given as a function of insolation, using generating efficiencies as parameters. Finally, a typical daily energy production is computed.

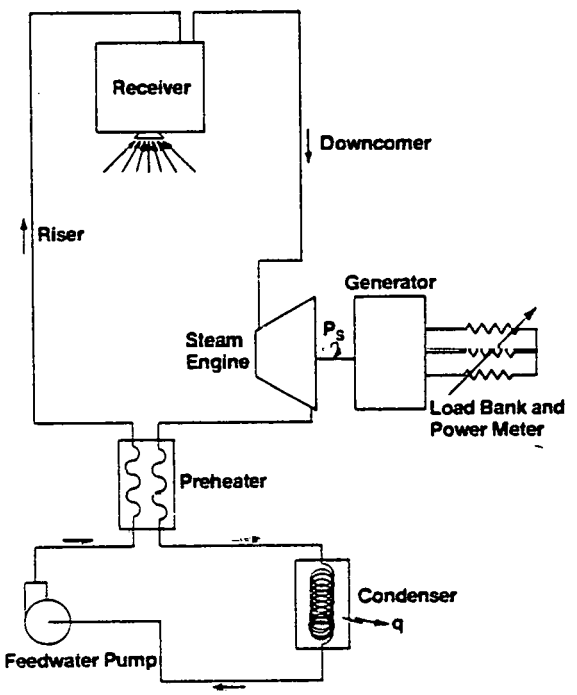

Figure 1a. Steam Loop Schematic

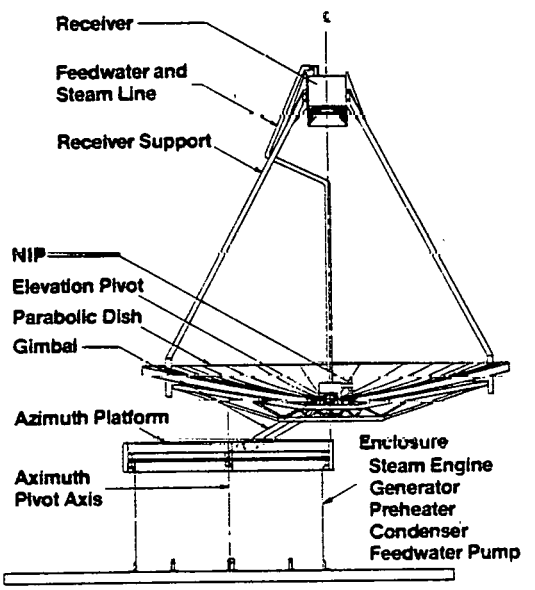

Figure 1b. Heliodyne Tracking Concentrating Collector

DETERMINATION OF ELECTRICAL POWER OUTPUT

We measured the ability of the optical concentrator and thermal receiver to convert solar energy into thermal energy and to deliver this energy to the steam engine. Electrical power output could then be determined for a specific steam engine/electrical generator combination by specifying the efficiencies of these components.

Referring to Figure 1a, we define the efficiency of the steam cycle as the ratio of the engine shaft power P_s to the net rate at which energy is added by the concentrator/receiver to the working fluid (q_h):

$$\eta_{cy} = \frac{P_s}{q_h} \qquad (1)$$

If the electrical generator efficiency η_{gen} is the ratio of electrical power output P_e to the engine shaft power, then

$$P_e = q_h \, \eta_{cy} \, \eta_{gen} \qquad (2)$$

The net rate at which energy is added to the working fluid depends on how much of the solar energy incident upon the dish aperture area is focused into the receiver aperture, converted to thermal energy, and delivered to the steam engine. The net gain of optical energy by the receiver is expressed by

$$q_o = I_\sigma A_{dish}\left(1 - \frac{A_{block}}{A_{dish}}\right)\overline{\rho}_d \, \eta_\sigma (1 - \rho_{cav}) \qquad (3)$$

The optical efficiency is

$$\eta_{op} = \frac{q_o}{I_\sigma A_{dish}} \qquad (4)$$

The net enthalpy increase of the working fluid is q_o minus the energy loss to the ambient air due to conduction, convection, and radiation from the receiver (q_{rec}) and the downcomer (q_d). (The downcomer brings the working fluid to the steam engine from the receiver.) Thus, the enthalpy increase of the working fluid is

$$q_h = q_o - q_{rec} - q_d \qquad (5)$$

$$= \eta_{op} I_\sigma A_{dish} - q_{rec} - q_d$$

The electrical power output becomes

$$P_e = (\eta_{op} I_\sigma A_{dish} - q_{rec} - q_d)\eta_{cy} \, \eta_{gen} \qquad (6)$$

If the optical efficiency η_{op}, the receiver thermal loss q_{rec}, and the downcomer thermal loss q_d are determined, the electrical output of the system can be expressed as a function of the insolation, with the steam cycle efficiency and the electrical generating efficiency as parameters.

RECEIVER AND DOWNCOMER THERMAL LOSS

Because the receiver cavity operates well above ambient temperature, it is necessary to consider heat transfer from the receiver to the ambient air.

The receiver is shown in Figure 2 and is based upon an axisymmetric cavity of Inconel sheet formed into two cone-shaped surfaces. The ratio of cavity surface area to aperture area is 27.8. In thermal contact with the cavity is 33.71 kg. of 99.7% pure aluminum contained in a stainless steel pot. The feedwater enters the aluminum through a stainless steel tube 239 cm. long which coils through the aluminum mass and exits the receiver to carry the steam through the downcomer to the steam engine.

The cavity and thermal mass are insulated by a ceramic shell which, in turn, is surrounded by a blanket of mineral wool. A stainless steel shell covers the entire outer surface of the receiver except the aperture. Structural support is provided by eight stainless steel members welded to the stainless steel pot. These members join in four pairs at the outer stainless steel shell to

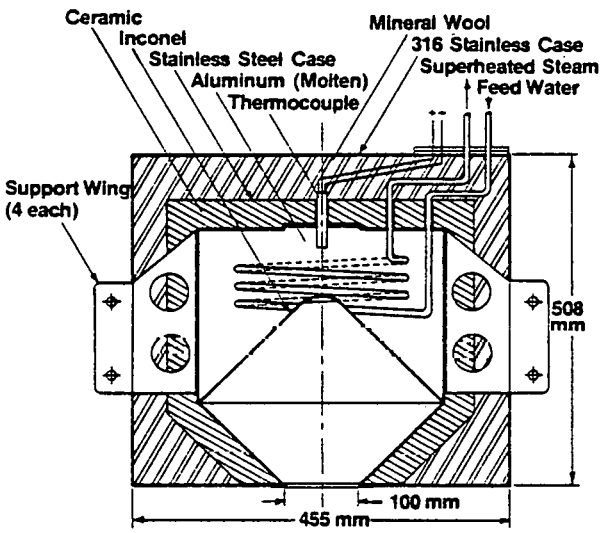

Figure 2. Receiver

form four flanges which bolt to the four receiver supports shown in Figure 1b. A thermocouple junction immersed in the aluminum block sends a signal to an electronic controller which ensures that the aluminum remains molten under normal operating conditions. Not shown in the figure is a device which protects the portion of the receiver facing the reflector. This device is a stainless steel screen which extends from the cylindrical part of the receiver about one receiver diameter along the optical axis and returns to the aperture of the receiver in the shape of a cone.

In order to analyze the receiver heat transfer, the various thermal resistances between the thermal mass and the ambient air must be determined. Included are the resistances of the ceramic and mineral wool insulation, the support wings, and the receiver supports. Radiation and convection from the receiver surface and radiation from the cavity should also be considered. A detailed analysis of each thermal resistance is beyond the scope of this paper but it is important to an understanding of the relative importance of the various heat loss mechanisms in the receiver. We will report the detailed analysis in the near future; here we present results of an experiment which directly determined the total thermal loss of the receiver under normal operating conditions.

The experiment took advantage of the fact that the thermal mass in the receiver is molten aluminum. Because the mass and composition of the aluminum are known quite accurately, the energy stored in the latent heat of fusion of the mass, H_f, is known. If the thermal mass is allowed to cool so that the aluminum freezes, then the amount of energy removed from the mass is H_f. If no insulation is present and if the feed water flow rate is zero, the only mechanism for removing H_f is the thermal loss of the receiver. In addition, while the aluminum is freezing the temperature of the thermal mass is fixed at the melting temperature (T_m = 660°C.), which is close to the normal operating temperature (typically 690°C.) and the temperature distribution is very nearly that within the receiver during normal operation. The only measurement required is a continuous record of the aluminum temperature. The period of time τ_f during which the aluminum temperature is constant gives the rate of heat loss:

$$q = \frac{H_f}{\tau_f} \qquad (7)$$

Since the receiver operates over a relatively narrow temperature range, a heat loss coefficient can be assumed independent of operating temperature:

$$U_r = \frac{H_f / \tau_f}{T_m - T_a} \qquad (8)$$

which, for any receiver operating temperature T_r gives the receiver loss

$$q_{rec} = U_r (T_r - T_a) \qquad (9)$$

where T_a is the ambient temperature.

For this experiment the aluminum temperature

(read by the thermocouple immersed in the thermal mass) was monitored on a strip-chart recorder. The temperature traces before and after the freezing period were extrapolated to determine the end points of the freezing period with maximum accuracy. Ambient temperature and wind speed were also monitored. The freezing process required 2.62 hr. at an average ambient temperature of 4° C. and an average wind speed of 1.9 meters/sec. The energy H_f dissipated during this time was 3699 w.-hr., which gives

$$U_r = 2.15 \qquad (10)$$

Thus, the receiver loss in watts can be expressed as

$$q_{rec} = 2.15\ (T_r - T_a) \qquad (11)$$

With the assumption that the cavity radiates as a blackbody, the radiation loss is 23% of the total receiver thermal loss. Thus, 77% of the receiver losses are due to conduction losses through the interior of the receiver.

The downcomer consists of a 7.62-cm. I.D. aluminum tube filled with mineral wool. The 0.70-cm. I.D. stainless steel steam line runs down the center of this tube, and the length from the receiver to the steam engine is 6.71 meters.

The steam temperature at the downcomer inlet is essentially the receiver temperature T_r because nearly all (85%) of the 2.4-meter steam line in the receiver is used for super heating. This was verified by a numerical model of the heat transfer in this "boiler" that allowed for variable fluid properties as a function of temperature. The model showed that the steam temperature was usually within 95% of the receiver temperature (referenced to feedwater temperature at the receiver inlet) after traversing 52% of the path in the receiver. The thermal loss from this insulated steam line can be calculated using the steam flow rate and the steam temperature at the receiver outlet (T_r). For the expected range of feedwater flow rates (18 to 40 kg./hr.), the analysis of the loss from the downcomer gives

$$q_d = 1.39\ (T_r - T_a) \qquad (12)$$

OPTICAL EFFICIENCY

The optical efficiency was determined from measurements of the time required to fully melt the aluminum mass and the insolation during this period. From Equations (3) and (4), the optical energy input to the receiver during this period is

$$\int \eta_{op}\ I_o\ A_{dish}\ dt \qquad (13)$$

This energy is partially stored in the thermal mass and partially lost to ambient air:

$$\int \eta_{op} I_\sigma A_{dish}\ dt = H_f + \int U_r\ (T_m - T_a)\ dt \qquad (14)$$

Given the ambient wind speed, U_r is known from the thermal loss experiments. By monitoring T_a during the experiment we were able to compute an average optical efficiency from

$$\eta_{op} = \frac{H_f + \int U_r\ (T_m - T_a)\ dt}{\int I_\sigma A_{dish}\ dt} \qquad (15)$$

Note that the optical efficiency is actually not constant because the dish motions (due to winds and tracking errors) cause η_σ in Equation (3) to vary as the energy spillage at the receiver aperture varies; however, the time constant of these fluctuations is a much shorter than the time constant of the thermal mass. Therefore, the optical efficiency measured this way is meaningful if the ambient winds are relatively uniform during the experiment. The optical efficiency then becomes a function of average ambient wind speed.

During this experiment, 0.335 hr. was required to melt the aluminum. The average ambient temperature was 2° C. and the average wind speed was 1.3 meters/sec. Total beam insolation during this period was 337 w.-hr./meter^2.

Using the loss coefficient from Equation (10) in Equation (15) gives

$$\eta_{op} = 0.44 \qquad (16)$$

It is possible at this time to determine A_{block} and $\overline{\rho}_d$. The area of the dish which is shaded or does not reflect light is

$$A_{block} = 1.46 \text{ meter}^2 \qquad (17)$$

which includes a central obstruction of 1-meter diameter and radial gaps of 1.5-cm. width between the 18 reflector petals.

The value in Reference 8 for the effective surface reflectance of Alzak sheet within the receiver acceptance angle (25 mrad.) is

$$\overline{\rho}_d = 0.77 \qquad (18)$$

Using these values of $\overline{\rho}_d$, A_{block} and η_{op} in Equation 3 gives

$$\eta_\sigma (1 - \rho_{cav}) = 0.60 \qquad (19)$$

This does not agree with results calculated in Reference 9 for point focus collectors with cavity receivers. In Reference 9, the "collector efficiency" is computed for a range of receiver temperature, cavity surface area to cavity aperture area ratio, cavity emittance, and concentrator slope error. This efficiency, written in our notation, is

$$\eta = \eta_\sigma (1 - \rho_{cav}) - \frac{q_{rec}}{\overline{\rho}_d I_o (A_{dish} - A_{block})} \qquad (20)$$

and for low receiver temperatures, q_{rec} is negligible so that

$$\eta = \eta_\sigma (1 - \rho_{cav}), \; T_r \longrightarrow T_a \qquad (21)$$

In this limit η becomes relatively insensitive to the other collector parameters and we find that our estimate of $\eta_\sigma(1 - \rho_{cav}) = 0.60$ is much less than the value of approximately 0.96 predicted by Reference 9.

Factors which degraded the measured optical efficiency beyond that predicted in Reference 9 were deposits on the reflecting surface (which reduce η_σ significantly below the value for a clean surface of 0.77) and gross focusing errors, which are apparently caused by poor adjustment of the 18 reflector petals. These gross focusing errors were obviously a major source of the optical losses. During these experiments the focused energy covered an area about twice the area of the receiver aperture. At this point, it is not clear whether better adjustment of the reflector petals would bring $\eta_\sigma(1 - \rho_{cav})$ closer to 0.96.

CALCULATION OF ELECTRICAL POWER OUTPUT

To determine the electrical power output, η_{op}, q_{rec} and q_d are inserted into Equation (6). Typical operation temperature in the receiver is 690°C. Assuming ambient temperature of 0°C. and ambient wind speed of 1.5 meter/sec., we find from Equations (11), (12), and (16)

$$P_e = (12.38 \, I_o - 2443) \, \eta_{cy} \eta_{gen} \qquad (22)$$

The quantity $P_e / \eta_{cy} \eta_{gen}$ is plotted in Figure 3 and is actually the net thermal power added to the working fluid by the solar collector and delivered to the steam engine. For an example of electrical power output, assume an electrical generator efficiency of 80% and a cycle efficiency which is 50% of Carnot (based on receiver temperature = 690°C. and ambient temperature = 0°C.) so that

$$P_e = 3.55 \, I_o - 701 \qquad (23)$$

For an insolation of 940 w./meter^2 we find $P_e = 2639$ w.

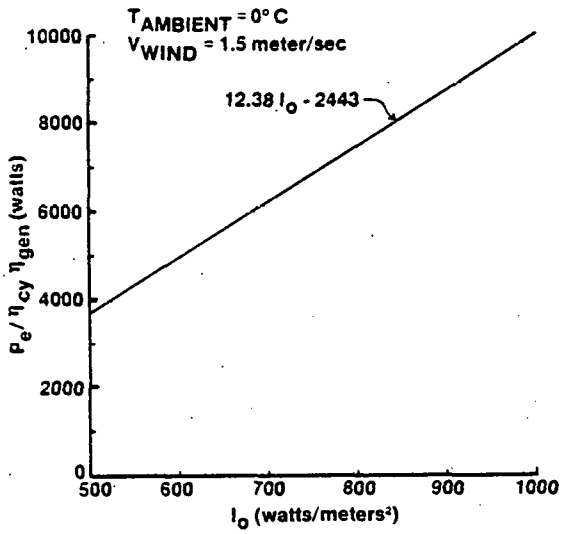

Figure 3. Electrical Power Output vs. Beam Insolation

Based upon a solar energy input $I_o A_{dish}$ of 26,578 w., the relative magnitudes of the various losses at this operating point are as given in Table 1.

In addition, it is worth noting that the feedpump consumes about 100 w. and that about 50 w. is required to operate the tracking mechanism.

Using Equation (23) and insolation data for a given location, we can calculate the daily electrical energy production by the system on a day of clear sunshine. For example, consider insolation data from Reference 7 for 40° N latitude, January 21. Energy production can be calculated from

$$E = \int_{day} P_e\,(t)\,dt \qquad (24)$$

where $P_e(t)$ is calculated from Equation (23) using $I_o(t)$ from Reference 7. This gives E = 17340 w.-hr. In a similar manner, insolation data for any locale or cloudiness condition could be inserted in Equation (23) to give energy production. The insolation data, however, should be beam insolation within the acceptance angle (1.43 deg.) of this concentrator.

CONCLUSIONS

This concentrator/receiver is capable of delivering 9194 w. of thermal energy to the steam engine at a level of insolation of 940 w./meter^2. In general, the delivered thermal energy is

$$q_h = 12.38\ I_o - 2443 \qquad (25)$$

which represents about 35% of the solar energy input. Improper adjustment of the dish reflector petals is probably the major source of optical energy losses. Thermal losses from the receiver and downcomer contribute a 9% loss of the solar energy. Assuming typical values for the steam cycle efficiency and electrical generator efficiency, the system should produce

Table 1. SYSTEM LOSSES FOR 26578 w. INPUT

	Loss (w.)	% of Input
Optical loss		
Surface reflectance, area blockage and shading	7170	27
Slope, aiming and tracking errors and cavity reflectance	7763	29
Receiver thermal loss	1484	5.6
Downcomer thermal loss	959	3.6
Steam cycle loss (assumed)	5905	22
Electrical generator loss (assumed)	659	2.5
Net power produced	2639	9.9

2639 w. of electrical power at peak insolation, and on a clear winter day at the test site it should produce 17.34 kw_e-hr.

ACKNOWLEDGEMENTS

The participation in the early phases of this work and the continued support throughout the effort by the following SERI staff members is greatly appreciated: Frank Kreith, Bim Gupta, Charles Benham, Paul Bergeron, and Dean Stansbury.

The assistance of the Tests and Measurements Group at SERI is also acknowledged.

This paper is an account of work under the SERI Solar Thermal Program. SERI is operated by the Midwest Research Institute for the U.S. Department of Energy.

NOTATION

A_{block}	Area of concentrator which is shaded or does not reflect light (meter^2).
A_{dish}	Circular area of concentrator defined by dish diameter (meter^2).
E	Electrical energy produced in one day (w. - hr.).
H_f	Heat of fusion of the thermal mass (w. - hr.).
I_o	Beam insolation (w./meter^2).
P_e	Instantaneous electrical power output (w.).
P_s	Power at steam engine shaft (w.).
q_d	Downcomer thermal loss (w.).
q_h	Net rate at which energy is added to working fluid and delivered to steam engine (w.).
q_o	Net rate of optical energy gain by receiver (w.).
q_{rec}	Receiver thermal loss (w.).
t	Time (hr.).
T_a	Ambient temperature (°C.).
T_m	Melting temperature of thermal mass (°C.).
T_r	Temperature of thermal mass (°C.).
U_r	Receiver loss coefficient (w./°C.).
η	Collector efficiency, used in Reference 8.
η_{cy}	Steam cycle efficiency, Equation (1).
η_{gen}	Electrical generator efficiency.
η_{op}	Optical efficiency, Equation (4).
η_σ	Fraction of optical energy approaching receiver which enters receiver aperture.
ρ_{cav}	Fraction of optical energy entering receiver aperture which is reflected out of the receiver.
$\overline{\rho_d}$	Reflectance of dish surface within collector acceptance angle.
τ_f	Time required for thermal mass to freeze (hr.).

LITERATURE CITED

1. Ramsey, J. W., J. T. Barzoni, and T. H. Hollands, NASA Report CR-134804 (1975).
2. Simon, F. F., Solar Energy, 18, 451-66 (1976).
3. Kumar, S., and H. J. Liers, ASME Paper 76-WA/HT-27 (1976).
4. Kreith, F., ASTM Stand. News, 3, 30-6 (1975).
5. Hill, J. E., and E. R. Streed, Solar Energy, 18, 421-31 (1976).

6. Ramsey, J. W., B. P. Gupta, and G. R. Knowles, ASME Journal of Heat Transfer, 99, 163-8 (May 1977).

7. Kreith, F., and J. Kreider, Principles of Solar Engineering, Hemisphere Publishing Co., Washington, D.C. (1978), p. 672.

8. Pettit, Richard B., SAND 76 0573.

9. Wu, Y. C., and L. C. Wen, ASME Paper 78-WA/Sol-5 (1976).

SERI

DISTRIBUTION LIST

No. of Copies	Distribution
1	Department of Energy: DOE, SERI Site Office Contracting Officer Attn: Charles M. Skinner
1	Chicago Operations Office Interim Program Division Attn: M. E. Jackson
1	Division of Solar Technology Office of Asst. Director for Administration Attn: R. H. Annan
1	Office of Asst. Secretary for Conservation & Solar Applications Attn: R. Scott
1	Office of Solar, Geothermal, Electric & Storage Programs Attn: Martin Adams
1	Division of Energy Technology Administration Attn: S. Hansen
1	Division of Distributed Solar Technology Office of the Director Attn: R. San Martin
1	Division of Central Solar Technology Office of the Director Attn: H. Coleman
1	Division of Energy Storage Systems, ETS Office of the Director Attn: G. Pezdirtz
1	Division of Planning & Energy Transfer, ETS Office of the Director Attn: Leslie Levine
1	Wind Energy Systems Attn: L. Divone